Connection of gamma rays, dark matter, and Higgs boson searches at the LHC

J. D. Ruiz-Alvarez,[2,*] C. A. de S. Pires,[1,†] Farinaldo S. Queiroz,[1,3,‡] D. Restrepo,[2,§] and P. S. Rodrigues da Silva[1,‖]

[1]*Departamento de Física, Universidade Federal da Paraíba, Caixa Postal 5008, 58051-970, João Pessoa, Paraiba, Brazil*

[2]*Instituto de Fisica, Universidad de Antioquia, A.A. 1226, Medellin, Colombia*

[3]*Fermi National Accelerator Laboratory, Center for Particle Astrophysics, Batavia, Illinois 60510, USA*

(Received 25 June 2012; revised manuscript received 22 August 2012; published 8 October 2012)

Motivated by the upcoming Higgs analyses, we investigate the importance of the complementarity of the Higgs boson chase on the low-mass weakly interacting massive particle (WIMP) search in direct detection experiments and the gamma-ray emission from the Galactic Center measured by the Fermi-LAT telescope in the context of the $SU(3)_c \otimes SU(3)_L \otimes U(1)_N$. We obtain the relic abundance, thermal cross section, and the WIMP-nucleon cross section in the low-mass regime and network them with the branching ratios (BRs) of the Higgs boson in the model. We conclude that the Higgs boson search has a profound connection to the dark matter problem in our model, in particular for the case that ($M_{\rm WIMP} <$ 60 GeV) the BR($H \rightarrow 2\,{\rm WIMPs}$) $\gtrsim 90\%$. This scenario could explain the gamma-ray emission from the Galactic Center observed by the Fermi-LAT telescope through the $b\bar{b}$ channel with a WIMP in the mass range of 25–45 GeV, while still being consistent with the current limits from XENON100 and CDMSII. However, after the recent LHC measurements concerning the Higgs, this window has been completely forfended, implying that $M_{\rm WIMP} > M_H/2$ and, consequently, ruling out any attempt to explain the Fermi-LAT observations, although still offering a region of the parameter space consistent with the current bounds. Lastly, we show that our model has a Standard Model-like Higgs boson for the regime that $M_{\rm WIMP} > M_H/2$, by computing the BRs into bb, $\gamma\gamma$ and $\tau\tau$.

DOI: 10.1103/PhysRevD.86.075011 PACS numbers: 12.60.−i, 12.60.Fr, 14.80.Bn

I. INTRODUCTION

The nature of the dark matter (DM) is one of the biggest mysteries of the universe and lies on the interface of particle physics, astrophysics and cosmology. It is common sense that in order to determine its nature, a complementary search in direct and indirect detection plus collider experiments is necessary. The long standing DAMA/LIBRA experiment reports with significance of 8.9σ the detection of an annual modulation with a phase and period consistent with elastically scattering dark matter, a WIMP [1] with a mass of $\sim$7 GeV, with a WIMP-nucleon cross section of $\sim 10^{-41}$ cm^2 [2]. The CRESST and CoGeNT experiments observed recently some excess events consistent with WIMP scattering off a nuclei with a similar spectrum of events [3,4]. The CoGeNT Collaboration has reported an annual modulation with an amplitude higher than DAMA but also consistent with the WIMP hypothesis. Those observations seem to point to an imminent WIMP discovery in the near future. However, the DAMA modulation is arguable since there are analyses which claim that this modulation could be due to cosmic ray muons [5], while others disagree with the muon hypothesis by declaring that the phases are $\sim 5\sigma$ off [6] and the scattering rates are different. With respect to the CoGeNT excesses, the uncertainties in the rise time cut may result in a sizable contamination of surface events in CoGeNT data and, therefore, a fraction of these excess events is expected to be residual surface events [2]. Lately, a large background contamination is expected in the CRESST detector by ^{206}Pb decays and α particles [7]. Furthermore, these signals appear to be in conflict with the other experiments, such as CDMSII and XENON10. In particular, the CDMS Collaboration has searched for this modulation in their last run but no annual modulation was found [8]. Conversely, the XENON detector which measures ionization and scintillation and has the strongest constraints in this mass range, suffers non-negligible uncertainties in the scintillation efficiency at low recoil energies as discussed in Ref. [9], making it difficult to interpret their resulting limits at low-energy range. Likewise, it is important to mention that at such low energies, the backgrounds observed by CDMS are not well understood, somewhat limiting their ability to probe the region implied by CoGeNT and DAMA/LIBRA [10]. Be that as it may, one could evoke non-Maxwellian distributions and/or tidal streams to alleviate the tension among those experiments [11]. In summary, the question of whether these signals reported recently are due to dark matter or not is still debatable. Besides this search for dark matter at low-energy recoils, an important and enlightening monophoton and monojet search has been performed at the LHC and the strongest limits in the $\sim$1 GeV mass window have been put for the case of light mediators [12]. Furthermore, important analyses have been performed on the Higgs-WIMP relation, in particular investigating the impact of the LHC results concerning the Higgs

*jose@gfif.udea.edu.co.
†cpires@fisica.ufpb.br
‡fqueiroz@fnal.gov
§restrepo@udea.edu.co
‖psilva@fisica.ufpb.br

on the WIMP search [13]. Moreover, an interesting and promising search for dark matter is ongoing in a variety of ground-based and space- based telescopes [14]. In particular, the Fermi Gamma Ray Space Telescope has been collecting data for four years from the region surrounding the center of the Milky Way, which is astrophysically both rich and complex and is predicted to contain very high densities of dark matter. By analyzing the morphology and spectrum of the gamma-ray emission from this region, several groups [15,16] have found evidence of a spatially extended component that peaks at energies between 300 MeV and 10 GeV which can be explained either by the annihilations of dark matter particles in the inner galaxy or by the collisions of high-energy protons (that are accelerated by the Milky Way's supermassive black hole) with gas. If interpreted as dark matter annihilation products, the emission spectrum favors dark matter particles with a mass in the range of (25–45) GeV, which annihilates mainly to $b\bar{b}$ (see Fig. 6 of Ref. [16]). Besides all these direct and indirect detection signals, we have the ongoing Higgs analyses that soon will shed some light in the new physics models [17]. Here, we explore the complementarity of these three approaches in the context of the $SU(3)_C \otimes SU(3)_L \otimes U(1)_N$, 3-3-1LHN for short [18–21]. Besides featuring many of the standard model (SM) virtues, it addresses fundamental questions such as the dark matter signals [22] as well as many theoretical questions, such as number of families [18] and neutrino masses, among others [20]. We will not dwell on the nice features of the model, but we recommend those works aforementioned for those who are interested in more detailed descriptions. Despite the fact that the cold dark matter problem has been previously investigated in the context of 3-3-1 models in Ref. [22], here we will also investigate indirect detection signals, derive the branching ratios (BRs) of the Higgs boson into WIMPs, $b\bar{b}$, $\gamma\gamma$ and $\tau\bar{\tau}$, and examine the role of the Higgs boson in direct and indirect detection searches by analyzing the impact of the ongoing Higgs boson chase on the parameter space of the model, so as to explain the gamma-ray emission from the Galactic Center (GC), while obeying the current bounds coming from direct detection experiments such as XENON100 and CDMSII.

We briefly describe the model in Sec. II by introducing its main ingredients. In Sec. III, we discuss in more detail the direct and indirect evidence for dark matter as well as our reasoning. Further, in Sec. IV, we discuss the impact of the Higgs boson search on our results and relate them to the dark matter problem. Lastly, we present our conclusions.

II. THE 3-3-1 LEFT-HANDED NEUTRINO MODEL

Our framework is the 3-3-1LHN model [18], which is a direct extension of the electroweak sector of the SM. In order to allow the reader to follow our reasoning, we will briefly discuss the content of the model hereafter.

A. Fermionic content

As in the SM, the leptonic sector is placed with left-handed fields appearing in triplets, $f_{aL} = (\nu_L^a, l_L^a, N_L^a)^T$ transforming as $(1, 3, -1/3)$, and right-handed ones in singlets, e_{aR} as $(1, 1, -1)$ and N_R^a as (1,1,0), where $a = 1, 2, 3$ corresponds to the three families. In the hadronic sector, the first two families are placed as antitriplets $Q_{iL} = (d_{iL}, -u_{iL}, d'_{iL})^T$ as $(3, \bar{3}, 0)$, with $i = 1, 2$, while the third one is arranged as triplet, $Q_{3L} = (u_{3L}, d_{3L}, u'_{3L})^T$ as $(3, 3, 1/3)$, and the right-handed quarks are singlets with hypercharges equal to their electric charges similarly to the SM. The first two and the third family of left-handed quarks are in different representations due to an anomaly cancellation requirement adequately described in previous works [18]. The primed fermions are the exotic ones—singlets under the SM gauge group. Similarly to the SM, all fermions acquire Dirac mass terms through a spontaneous symmetry-breaking mechanism in the Higgs sector presented hereafter.

B. Scalar content

It was noticed that by introducing a global symmetry $U(1)_G$, where

$$\mathbf{G}(\bar{N}_{L/R}, \bar{u}'_{3L/R}, d'_{iL/R}, V_\mu^-, U_\mu^0, \chi^0, \chi^-, \eta'^{0*}, \rho'^-) = +1, \quad (1)$$

we could simplify our model and, in addition, obtain the lightest particle charged under this symmetry to be stable. This procedure was already discussed in detail in Ref. [22]; hence, we skip it here. In summary, we introduce three scalar triplets, namely,

$$\chi = (\chi^0, \chi^-, \chi'^0)^T, \qquad \rho = (\rho^+, \rho^0, \rho'^+)^T, \qquad \eta = (\eta^0, \eta^-, \eta'^0)^T, \quad (2)$$

along with the following Yukawa Lagrangian,

$$\begin{aligned} -\mathcal{L}^Y = {} & f_{ij}\bar{Q}_{iL}\chi^* d'_{jR} + f_{33}\bar{Q}_{3L}\chi u'_{3R} + g_{ia}\bar{Q}_{iL}\eta^* d_{aR} \\ & + h_{3a}\bar{Q}_{3L}\eta u_{aR} + g_{3a}\bar{Q}_{3L}\rho d_{aR} + h_{ia}\bar{Q}_{iL}\rho^* u_{aR} \\ & + G_{ab}\bar{f}_{aL}\rho e_{bR} + g'_{ab}\bar{f}_{aL}\chi N_{bR} + \text{H.c}, \end{aligned} \quad (3)$$

with the triplets η and χ both transforming as $(1, 3, -1/3)$ and ρ as $(1, 3, 2/3)$, and in Eq. (3) we are using the family indexes $i = 1, 2$ and $a = 1, 2, 3$.

The most general scalar potential that we can build, invariant under the gauge group and the above global symmetry, is

$$\begin{aligned} V(\eta, \rho, \chi) = {} & \mu_\chi^2\chi^2 + \mu_\eta^2\eta^2 + \mu_\rho^2\rho^2 + \lambda_1\chi^4 + \lambda_2\eta^4 \\ & + \lambda_3\rho^4 + \lambda_4(\chi^\dagger\chi)(\eta^\dagger\eta) + \lambda_5(\chi^\dagger\chi)(\rho^\dagger\rho) \\ & + \lambda_6(\eta^\dagger\eta)(\rho^\dagger\rho) + \lambda_7(\chi^\dagger\eta)(\eta^\dagger\chi) \\ & + \lambda_8(\chi^\dagger\rho)(\rho^\dagger\chi) + \lambda_9(\eta^\dagger\rho)(\rho^\dagger\eta) \\ & - \frac{f}{\sqrt{2}}\epsilon^{ijk}\eta_i\rho_j\chi_k + \text{H.c.} \end{aligned} \quad (4)$$

It is well known that this potential is appropriate to induce the desired spontaneous symmetry-breaking pattern of the electroweak gauge symmetry, $SU(3)_L \otimes U(1)_N$ to $SU(2)_L \otimes U(1)_Y$, and finally to $U(1)_{\rm QED}$, generating the masses of gauge bosons and fermions through the so-called Higgs mechanism.

C. Mass eigenstates

In order to achieve spontaneous symmetry breaking, we suppose that the neutral scalars $(\eta^0, \rho^0, \chi'^0)$ develop a vacuum expectation value (VEV) according to

$$\eta^0, \rho^0, \chi'^0 \to \frac{1}{\sqrt{2}}(v_{\eta,\rho,\chi'} + R_{\eta,\rho,\chi'} + iI_{\eta,\rho,\chi'}). \quad (5)$$

Regarding the spontaneous symmetry-breaking process, there are important facts that should be emphasized. First, the VEVs v_ρ and v_η ($\ll v_{\chi'}$) have to be at the electroweak breaking scale, $v \approx 246$ GeV, since they fix the Z and $W^\pm$ gauge boson masses exhibited further, related by $v_\eta^2 + v_\rho^2 = v^2$. Second, we make the reasonable and simplifying assumption that the remaining neutral scalars (η'^0, χ^0) do not develop VEVs.[1]

Lastly, although the trilinear coupling f in Eq. (4) is a free mass parameter, in this work we make the assumption that f is of the order of the 3-3-1 symmetry-breaking scale, i.e., $f = v_{\chi'}/2$, where $v_{\chi'}$ is assumed to be few TeV, in order to simplify the diagonalization procedure, as well as $\lambda_2 = \lambda_3 = \lambda_6$.

From the pattern of symmetry breaking aforementioned, no mixing appears among the new neutrinos with the standard ones, and all of them acquire Dirac mass terms. The standard neutrinos gain their tiny masses due to effective dimension-five operators [19]. All the other fermions have SM-like masses. Moreover, for the sake of simplicity, we consider that the mass matrix of the charged leptons, new neutrinos and new quarks all come in diagonal mass bases.

Therefore, in the vacuum structure in Eq. (5), the mass matrix of the new neutrinos and quarks take the form,

$$M_{Na} = \frac{g'_{aa}}{\sqrt{2}} v_{\chi'}, \quad (6)$$

and

$$M_{q'_a} = \frac{f_{aa}}{\sqrt{2}} v_{\chi'}, \quad (7)$$

with all nondiagonal couplings set to zero. In our analyses we allow the Yukawa couplings of the heavy neutrinos free to float (assuming their masses are always larger than the mass of our WIMP), but we fix the new quarks' masses at 800 GeV. The lightest sterile neutrino has its stability guaranteed by the global symmetry $U(1)_G$ and, therefore, is a CDM candidate. However, we will not explore this possibility here because it has a too large and excluded WIMP-nucleon cross section in the low-mass regime [22].

After the process of symmetry breaking, we end up with the mass eigenvectors in the basis $(R_{\chi'}, R_\eta, R_\rho)$,

$$S_1 = R_{\chi'}, \qquad S_2 = \frac{1}{\sqrt{2}}(R_\eta - R_\rho), \qquad H = \frac{1}{\sqrt{2}}(R_\eta + R_\rho), \quad (8)$$

with respective mass eigenvalues,

$$M^2_{S_1} = \frac{v^2}{4} + 2v^2_{\chi'}\lambda_1, \qquad M^2_{S_2} = \frac{1}{2}v^2_{\chi'}, \qquad M^2_H = 3\lambda_2 v^2, \quad (9)$$

and in the basis of complex neutral scalars, (χ^0, η'^{0*}), we get the mass eigenstate,

$$\phi = \frac{v}{v_{\chi'}\sqrt{1 + \frac{v^2}{v^2_{\chi'}}}}\chi^{0*} + \frac{1}{\sqrt{1 + \frac{v^2}{v^2_{\chi'}}}}\eta'^0, \quad (10)$$

with a mass given by,

$$M^2_\phi = \frac{(\lambda_7 + \frac{1}{2})}{2}[v^2 + v^2_{\chi'}]. \quad (11)$$

Observe that since ϕ is a complex field from a combination of χ^0 and η'^0 which obey the $U(1)_G$ symmetry as we can check in Eq. (1), ϕ is charged under this symmetry. Since we will consider it to be the lightest one in the spectrum, the scalar ϕ, which is a neutral particle, will have its stability guaranteed by this global symmetry and its mass determined by two free parameters shown in Eq. (11).

There are other scalars in the spectrum, however, they do not play any role in our analyses. Hence, we will skip them in our discussion, but the complete spectrum of this model was studied in Ref. [22].

Finally, from the gauge-invariant scalar kinetic terms (not shown here) and using Eq. (5), we easily obtain the gauge boson masses,

$$m^2_{W^\pm} = \frac{1}{4}g^2v^2, \quad m^2_Z = m^2_{W^\pm}/c^2_W,$$
$$m^2_{V^\pm} = m^2_{U^0} = \frac{1}{4}g^2(v^2_{\chi'} + v^2), \quad (12)$$
$$m^2_{Z'} = \frac{g^2}{4(3 - 4s^2_W)}\left[4c^2_W v^2_{\chi'} + \frac{v^2}{c^2_W} + \frac{v^2(1 - 2s^2_W)^2}{c^2_W}\right].$$

In summary, the most important feature of this model is that the $U(1)_G$ symmetry implies that the charged particles under this symmetry are produced in pairs, like R-parity in supersymmetric theories [23], and hence the lightest

[1] If we take nontrivial VEVs for these scalars, we would still obtain the complete mass spectrum of the model with only additional complexity in the mixing of gauge bosons and scalars. However, this would also break the $U(1)_G$ global symmetry, yielding an unwanted Goldstone boson in the spectrum.

typical 3-3-1LHN model's particle will be stable. In this way the model can provide two (nonsimultaneous) WIMP candidates, N_1 and ϕ, where N_1 is a heavy neutrino and ϕ is a complex neutral scalar, which arises from the combination of the χ^0 and $\eta^{0\prime}$ scalar fields after the diagonalization procedure [22].

Here we will explore only the case where the scalar ϕ is the dark matter candidate. The reason relies on the fact that the other possible WIMP, N_1, has an excluded WIMP-nucleon cross section in the low-mass regime, which is exactly the region of mass we are interested in this work. All this being said, we will use the terminology "WIMP" to refer to our scalar ϕ from now on. In the next section we will investigate the status of our model with respect to the direct and indirect detection searches of dark matter.

III. DIRECT AND INDIRECT DETECTION

Among the CDM candidates, the WIMPs are the most promising ones for providing a thermal cross section roughly at the electroweak scale, naturally leading to the appropriate relic density, because the current and next generation of direct and indirect detection experiments are sensitive to the parameter space on which most of the theoretical models rely. Before examining the status of our model concerning those searches, we will scan the parameter space of the model and check if our WIMP can account for the total observed dark matter abundance by computing,

$$\Omega h^2 = 2.742 \times 10^8 \frac{M_{\mathrm{WIMP}}}{\mathrm{GeV}} Y(T_0), \tag{13}$$

where $Y(T_0)$ is the number density over entropy evaluated today.

We used the MicrOMEGAs package, where we implemented the model, to take into account all the processes that contribute to the relic abundance of our WIMP, ϕ, automatically [24]. The main processes that contribute to the abundance of our WIMP ϕ are exhibited in Fig. 1.

In Fig. 2, we show the abundance of the WIMP as a function of its mass and in Fig. 3 as a function of the mass of the Higgs boson in the low-mass WIMP regime, $M_{\mathrm{WIMP}} < 80$ GeV, with the Higgs mass varying from

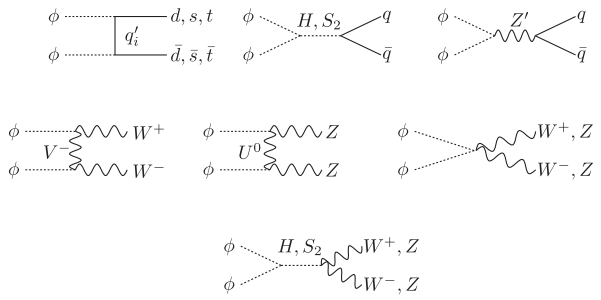

FIG. 1. The main processes that contribute to the abundance of ϕ.

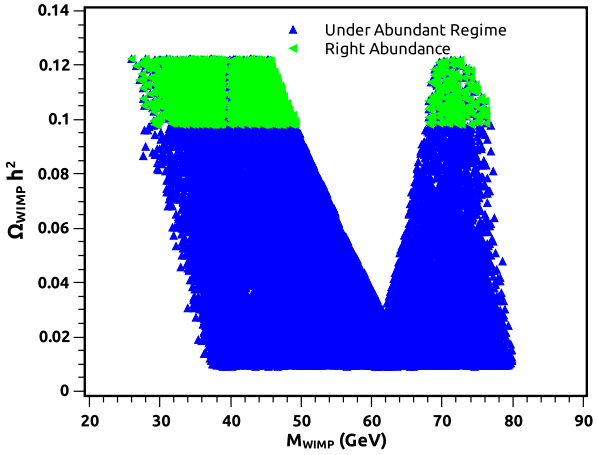

FIG. 2 (color online). Abundance of the WIMP (ϕ) as a function of its mass. Green (blue) scatter refers to points where the WIMP provides the correct abundance (is underabundant). Correct abundance means $0.098 \leq \Omega h^2 \leq 0.122$, while the underabundant regime is for $0.01 \leq \Omega h^2 \leq 0.098$. The Higgs mass is free to float in the 110–150 GeV.

110 up to 150 GeV. The results for higher masses are presented in Fig. 8 of Ref. [22], where it was concluded that there is a region of the parameter space for $M_{\mathrm{WIMP}} >$ 600 GeV that gives the right abundance while still being consistent with the current bounds.

From Fig. 2, we can clearly see that our model has a largish region where our WIMP, Φ, provides the right abundance according to WMAP7 [25]. Without any fine-tuning and with reasonable assumptions mentioned earlier, we can get $\Omega h^2 \sim 0.1$. Looking at the processes in Fig. 1, we see that the only free parameters that determine the abundance of our WIMP are the mass of the Higgs boson

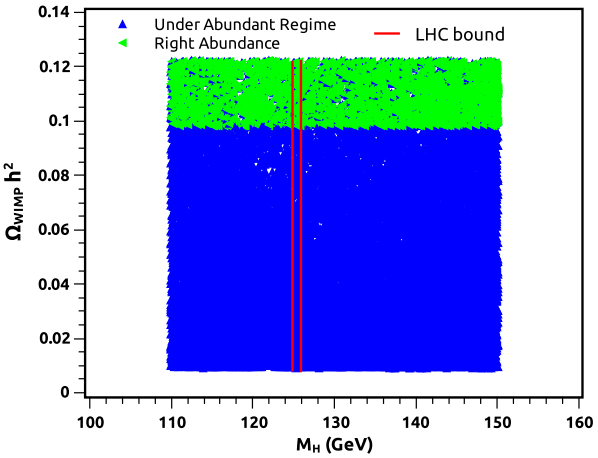

FIG. 3 (color online). Abundance of the WIMP (ϕ) as function of the Higgs boson mass (M_H). Green (blue) scatter refers to points where the WIMP provides the correct abundance (is underabundant). Correct abundance means $0.098 \leq \Omega h^2 \leq 0.122$, while the underabundant regime is for $0.01 \leq \Omega h^2 \leq 0.098$. We let 20 GeV $< M_{\mathrm{WIMP}} <$ 80 GeV.

and the scale of spontaneous symmetry breaking of the model, $v_{\chi'}$. The reason is that some processes involve gauge couplings, and the other couplings are strongly determined by the masses of the 3-3-1 particles that are controlled by $v_{\chi'}$.

Here, we leave $v_{\chi'}$ free to float between 14 TeV. These free parameters result in the scatters seen in Figs. 2 and 3. The most important contribution to the abundance is the Higgs-mediated process in Fig. 1. The thermal cross section for this process has a huge peak at $M_{\rm WIMP} \sim M_H/2$. This large cross section decreases the abundance proportionally in such a way that we enter the underabundant regime ($\Omega h^2 \sim 10^{-4}$) for $M_{\rm WIMP} \sim M_H/2$. Since we are scanning over 110 GeV $< M_H <$ 150 GeV, we end up with the V-shaped region in Fig. 2 around 50 GeV $\lesssim M_{\rm WIMP} \lesssim$ 70 GeV.

In Fig. 3, we have let the same parameters mentioned above float free and plotted the abundance in terms of the Higgs mass. We cannot see any bias towards a light Higgs boson ($M_H < 130$ GeV) and, therefore, by looking at the abundance dependence on the Higgs boson mass only, we cannot extract any information relevant to the Higgs boson search differently from some doublet Higgs models [26]. Nevertheless, it is evident that we have a WIMP that reproduces the right observed abundance and is in agreement with the recent findings of LHC, if the new particle is indeed a SM-like Higgs boson. That being said, we must then investigate if our model is also consistent with current limits from direct detection experiments.

Since we have a flux of WIMPs surrounding us, we expect to observe these WIMPs by detecting WIMP-nucleon scatterings in underground detectors. The measured quantities vary according to the detector technology; however, after making some assumptions concerning the dark matter distribution, all of them convert their results into the simple cross section (in the spin-independent case),

$$\sigma_0 = \frac{4\mu_r^2}{\pi}(Zf_p + (A - Z)f_n)^2, \tag{14}$$

where Z is the atomic number, A is the atomic mass and f_p and f_n are effective couplings with protons and neutrons, respectively, and depend on the particle physics input of a given model. It is important to emphasize that these couplings are obtained numerically in our model by the MicrOMEGAs package by following the recipe described in Ref. [24].

As aforementioned, the direct detection signals observed by CoGeNT, CRESST and DAMA may not be due to WIMP scatterings, so under the null hypothesis we are only concerned whether our WIMP candidate has a WIMP-nucleon cross section below the current bounds. In Fig. 4, we have shown all the processes which, in principle, contribute to the WIMP-nucleon cross section. The most relevant processes are the H-, S_2- and Z' mediated ones. Since we let their masses vary, we obtain the scatter plots in Figs. 5 and 6.

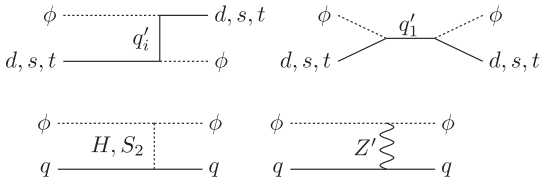

FIG. 4. Processes which contribute to the WIMP-nucleon cross section of ϕ.

In Figs. 5 and 6, we have plotted the WIMP-nucleon cross section as a function of the WIMP mass for the case that the Higgs varies in the 110–150 GeV mass range and for the case that $M_H = 125$ GeV. It may be noticed that the majority of the points are excluded by the recent XENON100 experiment; however, we still have a considerable region that is completely consistent with the current limits for $M_H = 125$ GeV. No fine-tuning was required to generate those plots. One can check that our model is completely consistent with a Higgs boson of $M_H = 125$ GeV.

It is important to emphasize, though, that the ongoing SuperCDMS at SNOWLAB, which will have a larger exposure by increasing the mass of the detector plus a better handle in discriminating surface events for implementing the new iZIP germanium detectors, and the XENON1T, for basically having a larger exposure, will be crucial to test our model in the near future, since they expect to improve their limits by roughly an order of magnitude.

In order to pin down the properties of the dark matter particle and find out the nature of the dark matter, we

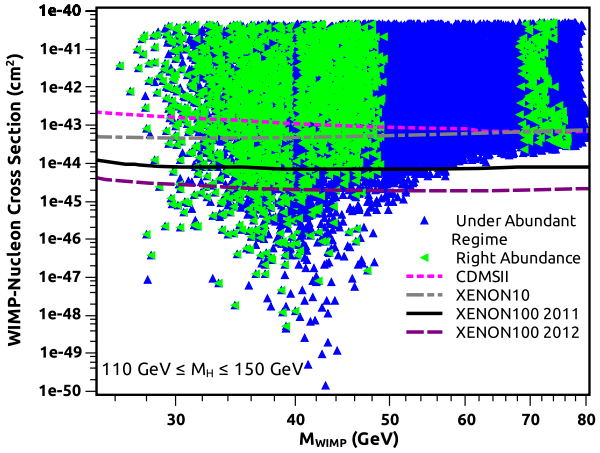

FIG. 5 (color online). WIMP-nucleon cross section as function of the WIMP mass. Green (blue) scatter refer to points where the WIMP provides the correct abundance (is underabundant). Correct abundance means $0.098 \leq \Omega h^2 \leq 0.122$, while the underabundant regime is for $0.01 \leq \Omega h^2 \leq 0.098$. We left the Higgs mass free to float in the 110 GeV $\leq M_H \leq$ 150 GeV.

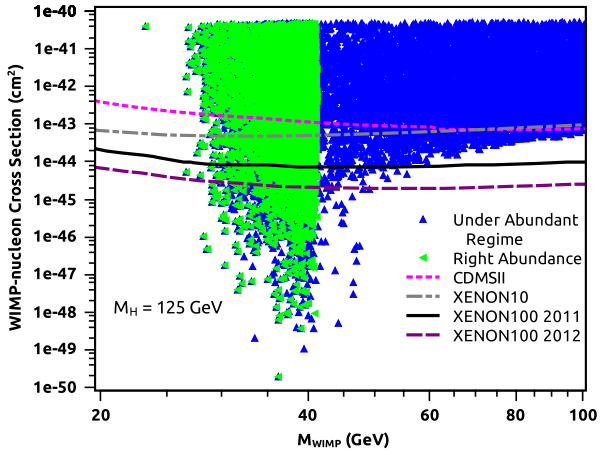

FIG. 6 (color online). WIMP-nucleon cross section as function of the WIMP mass for $M_H = 125$ GeV. Green (blue) scatter refer to points where the WIMP provides the correct abundance (is underabundant). Correct abundance means $0.098 \leq \Omega h^2 \leq 0.122$, while the underabundant regime is for $0.01 \leq \Omega h^2 \leq 0.098$. We let the WIMP mass vary in the 20–80 GeV mass range.

should also search for dark matter annihilations in our neighborhood. It has been thought that if a sizable fraction of dark matter particles can annihilate into a pair of SM particles, the Galactic Center would be one of the best places to search, since it would be the brightest in gamma-ray emission and provide better statistics.

The flux of gamma rays coming from DM annihilation is given by,

$$\phi_\gamma(E_\gamma, \psi) = \frac{dN_\gamma}{dE_\gamma} \frac{\langle \sigma v \rangle}{8\pi M^2_{\rm WIMP}} \int_{\rm los} \rho^2(r) dl, \qquad (15)$$

where $\langle \sigma v \rangle$ is the dark matter annihilation cross section times the relative velocity of the incoming WIMPs averaged over the velocity distribution, and ψ is the angle observed relative to the direction of the Galactic Center. The dark matter density as a function of distance to the GC is given by $\rho(r)$, and the integral is performed over the line of sight. $\frac{dN}{dE_\gamma}$ is the gamma-ray spectrum generated per annihilation.

In the right-hand side of Eq. (15), we have two different types of information. The integration is the astrophysical input. while the other terms refer to the particle physics information, and, therefore, are model dependent. It is noteworthy to point out that the particle physics information is essentially the mass of the dark matter particle and the value of the cross section into the final states we are interested in.

Hence, once you measure the flux and assume a dark matter distribution and decay mode, there are two free parameters left, which are the mass of the dark matter particle and the thermal cross section. Based on this information, we will investigate the possibility of explaining the gamma-ray emission from the GC in our model.

By analyzing the Fermi-LAT data from August 4, 2008, and August 3, 2011, and using the ULTRACLEAN class of events (events with less contamination of cosmic rays), a group has concluded that after subtracting the point source emission and the cosmic rays background, a residual emission from the inner five degrees surrounding the Galactic Center was present [16], which is in good agreement with previous works [15].

A number of proposals have been put forth to explain this gamma-ray emission. Since the morphology of the gamma-ray emission is not entirely pointlike, the black hole hypothesis might be ruled out, and because 44 out of 46 of the resolved millisecond pulsars by Fermi-LAT have a spectrum index larger than one, it is somewhat unlikely to explain this gamma-ray emission through millisecond pulsars. In order to explain this observed gamma-ray flux, a large population of pulsars with a hard spectral index (~ 1.0) would be required. As mentioned before, this is not supported by the current data.

By using a Navarro-Frank-White (NFW) [24] profile with an inner slope of $\gamma = 1.3$, which is suggested by cosmological simulations of Milky Way—sized halos [27], it was concluded that between 70 and 100% of this gamma-ray emission is due to dark matter annihilations. In order to explain this gamma-ray emission, a dark matter particle should annihilate mainly to $b\bar{b}$ and have a mass in the $\sim$(15–45 GeV) range as well as a thermally averaged annihilation cross section of 10^{-26} cm$^3/s$ represented in the green region in Fig. 7.

In Fig. 7, we show the thermal cross section of our WIMP candidate as a function of its mass for the case

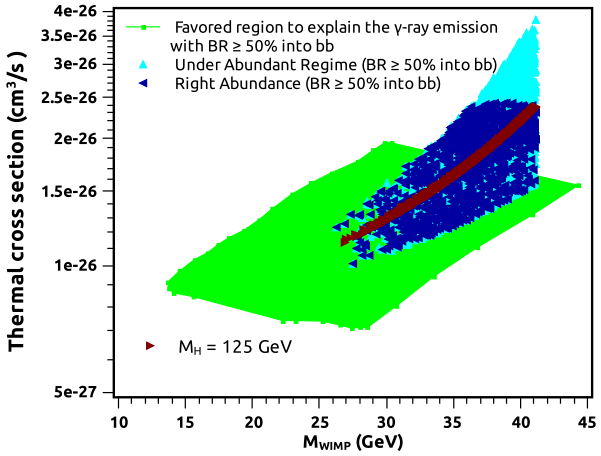

FIG. 7 (color online). Annihilation cross section as function of $M_{\rm WIMP}$ for $BR(b\bar{b}) \geq 50\%$. Green region represents the favored region by the gamma-ray emission detected by Fermi-LAT in the GC. Dark (light) blue points refer to the case where the WIMP provides the correct abundance (is underabundant). All (dark + light) blue points are for 110 GeV $\leq M_H \leq$ 150 GeV. The brown ones are for $M_H = 125$ GeV. Correct abundance means $0.098 \leq \Omega h^2 \leq 0.122$ while the underabundant regime is for $(0.01 \leq \Omega h^2 \leq 0.098)$. See the text for details.

that it annihilates dominantly to $b\bar{b}$ ($> 50\%$).[2] From Fig. 7, we notice that our WIMP might be the origin of the gamma-ray emission from the GC and, at the same time, explain the dark matter abundance indicated by WMAP7 within the ($25\ \text{GeV} \leq M_{\text{WIMP}} \leq 40\ \text{GeV}$) mass range.

So far we have proved that our model has a WIMP, which has a WIMP-nucleon cross section in the low-mass regime consistent with the current measurements regarding direct detection, and that it reproduces the right abundance indicated by WMAP7. Furthermore, we have shown that it can explain at least the majority of gamma-ray emission coming from the GC. Now, we will explore the complementarity of the ongoing Higgs boson search with the results we have discussed previously.

IV. HIGGS CONNECTION

Since we are at the LHC era, the complementarity has become a promising and achievable way to shed some light on new physics models and, most importantly, disentangle them from other models. Therefore, we will network the ongoing Higgs measurements with the gamma-ray emission from the Galactic Center and the bound coming from leading direct detection experiments, CDMS and XENON100.

The Higgs boson discovery is a major step forward in our understanding of how particles acquire mass [28]. Now that we have observed the Higgs boson, we must start studying its properties by measuring with high precision the decay channels in order to investigate to which model this Higgs belongs.

While at TEVATRON, the Higgs-associated production with $b\bar{b}$ in the final state is the most important channel to look for the Higgs; at the LHC, it is the Higgs production via gluon fusion with $\gamma\gamma$ in the final state because of its great invariant mass resolution and efficient background rejection. The recent excess observed in the $\gamma\gamma$ channel has lead to a greater focus on alternative theories that extend beyond the SM with Higgs-like particles such as the 3-3-1 class of models and supersymmetric models [17].

Similarly to many theories, when $M_{\text{WIMP}} < M_H/2$, the Higgs boson decays dominantly to a pair of DM particles, particularly WIMPs [29]. In Fig. 8, we exhibit the branching ratio for the Higgs boson into a pair of WIMPs as a function of the WIMP mass for different Higgs masses in the LHN model (see analytical expression in the Appendix).[3] We can confirm from Fig. 8 that the Higgs boson decays with a branching ratio larger than 90% into WIMPs.

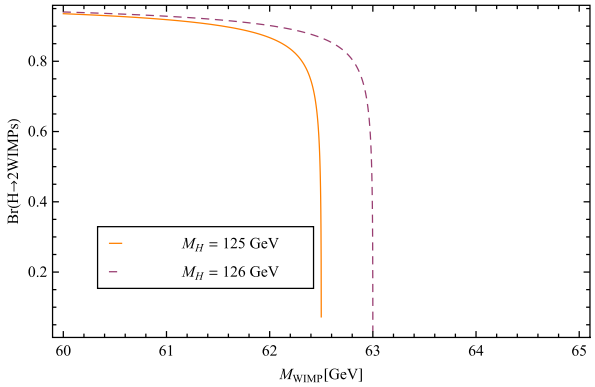

FIG. 8 (color online). Branching ratio of the Higgs boson into a pair of WIMPs. The solid thin orange line is for $M_H = 125$ GeV, the dashed purple line is for $M_H = 126$ GeV. For the case that $M_H = 125$ GeV and $M_{\text{WIMP}} = 62.5$ GeV, $BR(H \to \gamma\gamma) \simeq 1.45 \times 10^{-3}$, $BR(H \to b\bar{b}) \simeq 0.733$, and $BR(H \to \tau\bar{\tau}) \simeq 4 \times 10^{-2}$. We did not show these components in the plot for a matter of visualization.

In particular, for the case that $M_{\text{WIMP}} = 20$ GeV and $M_H = 125$ GeV, we obtained $BR(H \to \gamma\gamma) \simeq 2.9 \times 10^{-5}$ and $BR(H \to b\bar{b}) \simeq 1.4 \times 10^{-2}$, and $BR(H \to \tau\bar{\tau}) \simeq 7.9 \times 10^{-4}$. Similar suppressed branching ratios are found for the case that $M_{\text{WIMP}} < M_H/2$. Such a Higgs boson and DM connection is of the most relevant importance if we wish to address the issue of DM nature and its relation with electroweak physics. Our results reveal that a light scalar WIMP ($M_{\text{WIMP}} \leq 60$ GeV) in the 3-3-1LHN model is discarded in view of the recent LHC discovery [30], when we admit that the observed 125 GeV boson is SM-like Higgs.

Furthermore, the model is unable to support the DM hypothesis as an explanation for the gamma-ray emission from GC once this implies that $M_{\text{WIMP}} > 60$ GeV.[4] It is worth mentioning that for masses $\gg 60$ GeV, this model has a parameter space that evades the most stringent bounds as shown in Fig. 8, Ref. [22]. One may also wonder if the well measured invisible width of the Z boson could further constrain our model. Nevertheless, the Z boson cannot decay to WIMPs in our model simply because all the decay modes that involve a WIMP in the final state have at least one 3-3-1 particle that is much heavier than the Z boson.

Concerning the current ATLAS and CMS results [30], as the Higgs width to WIMPs falls rapidly as the WIMP mass gets closer to $M_H/2$, its decays are purely SM ones. Furthermore, we explicitly exhibit in the Figs. 9–11 that our model recovers the SM predictions regarding the Higgs branching ratios into $\gamma\gamma$, $b\bar{b}$ and $\tau\bar{\tau}$ for the case that $M_{\text{WIMP}} > M_H/2$, since from these plots we can clearly

[2]By modifying the main code in MicrOMEGAs, we where able to store only the points where the annihilation into $b\bar{b}$ was the dominant one.

[3]We have added all possible decay channels for the Higgs boson including radiative decays such as $Z\gamma$ in order to derive precise values for the branching ratios.

[4]We remark that this analysis was carried out prior to the boson discovery at LHC, and the null Higgs hypothesis was completely consistent with the measurements available then, since only a modest excess had been observed [31] with insufficient statistics to claim any strong evidence for the Higgs boson.

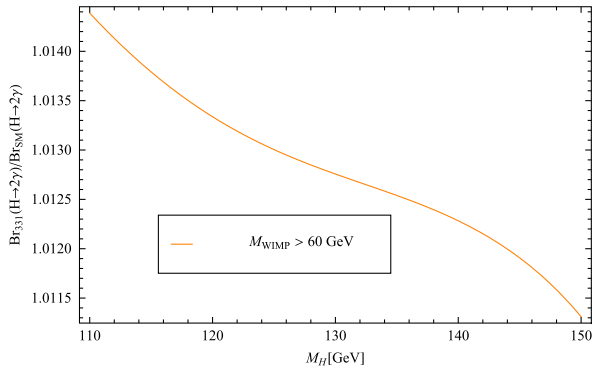

FIG. 9 (color online). Ratio of the branching ratios $H \to \gamma\gamma$ in the 3-3-1 model and in the SM for the case that $M_{\rm WIMP} > \frac{MH}{2}$.

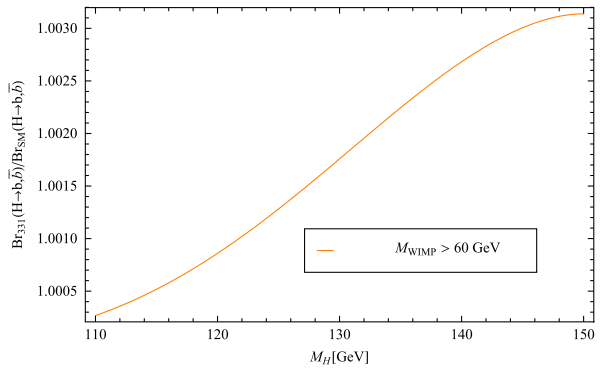

FIG. 10 (color online). Ratio of the branching ratios $H \to b\bar{b}$ in the 3-3-1 model and in the SM for the case that $M_{\rm WIMP} > \frac{MH}{2}$.

confirm that $BR_{331}/BR_{\rm SM} \simeq 1$. Therefore, in this regime our model has a SM-like Higgs boson. We have focused on these channels for simplicity and for being one of the most important ones for a light Higgs boson regarding the LHC measurements.

In summary, the ongoing precise measurements concerning the Higgs have a complementary and crucial role in identifying the nature of the dark matter in our model since the properties of the Higgs boson are tightly related to the mass of the DM particle in the 3-3-1LHN model.

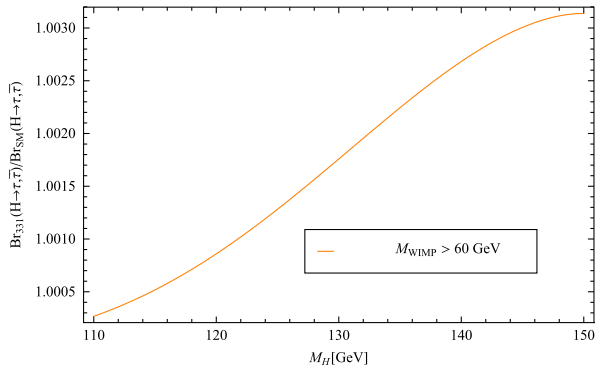

FIG. 11 (color online). Ratio of the branching ratios $H \to \tau\bar{\tau}$ in the 3-3-1 model and in the SM for the case that $M_{\rm WIMP} > \frac{MH}{2}$.

V. CONCLUSIONS

We have probed the low-mass WIMP window, $M_{\rm WIMP} < 60$ GeV, in the 3-3-1LHN model and checked if it can reproduce the right abundance of dark matter inferred by the WMAP7 satellite in Figs. 2 and 3. Subsequently, we have shown that a sizable region of the parameter space is constrained by the current bounds derived by the XENON100 and CDMSII Collaborations and a largish and promising region is completely consistent with those in Figs. 5 and 6. The upcoming XENON1T and SuperCDMS projected limits which are expected to improve by one order of magnitude their limits will be sensitive enough to further restrict our model or reveal its plausibility.

Moreover, we have discussed the possibility of explaining between 70% and 100% of the Fermi-LAT observed gamma-ray emission from the Galactic Center through a dominant annihilation into $b\bar{b}$ final states with a WIMP mass in the (25–40) GeV range in Fig. 7, showing that the 3-3-1LHN model has a large amount of parameter space to offer a plausible explanation for these events.

Additionally, we have networked the struggling probe for WIMPs in underground experiments with the ongoing Higgs boson measurements at Tevatron and LHC. We have obtained that there is a conflict between a WIMP light enough to explain the Fermi-LAT data and the 125 GeV Higgs-like boson discovered at LHC. The reason is that, for such a Higgs mass, there is a huge branching ratio to WIMPs in the 3-3-1LHNmodel, $BR(H \to 2WIMPs) \geq 90\%$; besides, the branching into a pair of photons is roughly two orders of magnitude smaller than the SM prediction, which is completely ruled out in view of the recent data. It represents a strong constraint to a light WIMP in this model, also frustrating to the explanation of the gamma-ray emission from GC observed at Fermi-LAT.

In order to avoid the Higgs decay into pair of WIMPs and increase the prediction to branching ratio into $\gamma\gamma$, we necessarily must take $M_{\rm WIMP} > M_H/2$ in the 3-3-1LHNmodel. We have shown in Figs. 9–11 that under the latter hypothesis, our model predicts no deviations from the SM Higgs boson decay channels.

We also remark that for the regime where $M_{\rm WIMP} < M_Z/2$, no bound can be derived regarding the Z boson invisible width because all decay modes that involve a WIMP in the final state have at least one 3-3-1 particle which is much heavier than the Z boson.

Finally, the analysis performed here has been very decisive in further scrutinizing the nature of DM we can have in the 3-3-1LHN and may even discard the model if future data reveals the existence of a WIMP lighter than $M_H/2$.

ACKNOWLEDGMENTS

We would like to thank Chris Kelso, Dan Hooper, LianTao, Daniele Alves, and A. Semenov as well as A. G. Dias for valuable discussions and/or comments.

C. A. S. P. and P. S. R. S. are supported by the Conselho Nacional de Desenvolvimento Científico e Tecnológico (CNPq), FSQ by Coordenação de aperfeiçoamento de Pessoal de Nível Superior (CAPES) and D. R. has been supported in part by UdeA/2011 Grant No. IN1614-CE.

APPENDIX

The invisible width $H \longrightarrow \text{WIMP} + \text{WIMP}$ in our model is given by

$$\Gamma_{\text{WIMP}} = \frac{\lambda^2_{(H\Phi\Phi)}}{32\pi}\frac{\sqrt{M_H^2 - 4M^2_{\text{WIMP}}}}{M_H^2}, \tag{A1}$$

where,

$$\lambda_{(H\Phi\Phi)} = \frac{-1}{\sqrt{2}(1+\frac{v^2}{V^2})}\left(3\lambda_2 v + \frac{v^3}{2V^2} + \lambda_7\frac{v^3}{V^2} + \lambda_7 v + \frac{v}{2}\right). \tag{A2}$$

WIMP refers to the scalar Φ in the model. Here $v = \frac{v_{SM}}{\sqrt{2}}$, and V is the scale of symmetry breaking of the 3-3-1 model, which we assume to be $\gtrsim 1$ TeV. Different values for V produce similar results.

It is important to notice that these couplings in Eq. (A2) are determined by the mass of the WIMP and Higgs boson, through the following equations,

$$M^2_{\text{WIMP}} = \frac{\lambda_7 + 1/2}{2}(v^2 + V^2), \tag{A3}$$

$$M_H^2 = 3\lambda_2 v^2. \tag{A4}$$

Therefore, fixing V in few TeV and plugging Eqs. (A2)–(A4) into Eq. (A1), we can express the invisible width as a function of the Higgs boson and WIMP masses only. For $M_H \sim 120$ GeV, and $20\ \text{GeV} \leq M_{\text{WIMP}} \leq 60$ GeV, the WIMP is the heaviest particle to which the Higgs can decay. For this reason, the BR of the Higgs boson into a pair of WIMPs is dominant in this mass range as we may observe in Fig. 8.

[1] R. Bernabei *et al.*, AIP Conf. Proc. **1417**, 12 (2011).
[2] C. Kelso, D. Hooper, and M. Bluckley, Phys. Rev. D **85**, 043515 (2012); J. Kopp, T. Schwetz, and J. Zupan, J. Cosmol. Astropart. Phys. 03 (2012) 001.
[3] CRESST Collaboration, Eur. Phys. J. C **72**, 1971 (2012); CoGeNT Collaboration, Phys. Rev. Lett. **106**, 131301 (2011).
[4] CoGeNT Collaboration, Phys. Rev. Lett. **107**, 141301 (2011).
[5] K. Blum, arXiv:1110.0857; J. P. Ralston, arXiv:1006.5255; D. Nygren, arXiv:1102.0815;
[6] R. Bernabei *et al.*, arXiv:1202.4179; J. Pradler, Eur. Phys. J. C **72**, 2064 (2012); C. Kelso and D. Hooper, Phys. Rev. D **84**, 083001 (2011).
[7] M. Kuzniak, M. G. Boulay, and T. Pollmann, Astropart. Phys. **36**, 77 (2012).
[8] CDMS Collaboration, arXiv:1203.1309.
[9] J. I. Collar, arXiv:1006.2031.
[10] J. I. Collar and N. E. Fields, arXiv:1204.3559.
[11] D. Hooper and C. Kelso, Phys. Rev. D **84**, 083001 (2011).
[12] Y. Gershtein, F. Petriello, S. Quackenbush, and K. M. Zurek, Phys. Rev. D **78**, 095002 (2008); CDF Collaboration, Phys. Rev. Lett. **108**, 211804 (2012).
[13] I. Low, P. Schwaller, G. Shaughnessy, and C. E. M. Wagner, Phys. Rev. D **85**, 015009 (2012); K. Belotsky, D. Fargion, M. Khlopov, R. Konoplich, and K. Shibaev, Phys. Rev. D **68**, 054027 (2003); C. W. Chiang, T. Nomura, and J. Tandean, arXiv:1205.6416; X. G. He, B. Ren, and J. Tandean, Phys. Rev. D **85**, 093019 (2012); X. G. He and J. Tandean, Phys. Rev. D **84**, 075018 (2011).
[14] VERITAS Collaboration, arXiv:0910.4563; M. Vivier, arXiv:1110.6615; H. E. S. S. Collaboration, Phys. Rev. Lett. **97**, 221102 (2006); H. E. S. S. Collaboration, Phys. Rev. Lett. **97**, 249901(E) (2006); K. N. Abazajian and J. Patrick Harding, J. Cosmol. Astropart. Phys. 01 (2012) 041; Fermi-LAT Collaboration, Astrophys. J. **747**, 121 (2012); A. V. Belikov, D. Hooper, and M. R. Buckley, Phys. Rev. D **86**, 043504 (2012).
[15] D. Hooper and L. Goodenough, Phys. Lett. B **697**, 412 (2011); M. Chernyakova, D. Malyshev, F. A. Aharonian, R. M. Crocker, and D. I. Jones, Astrophys. J. **726**, 60 (2011); A. Boyarsky, D. Malyshev, and O. Ruchayskiy, Phys. Lett. B **705**, 165 (2011).
[16] D. Hooper and T. Linden, Phys. Rev. D **84**, 123005 (2011).
[17] M. Carena, S. Gori, N. R. Shah, C. E. M. Wagner, and L.-T. Wang, J. High Energy Phys. 07 (2012) 175; H. An, T. Liu, and L.-T. Wang, arXiv:1207.2473; A. Alves, A. G. Dias, E. Ramirez Barreto, C. A. de S. Pires, F. S. Queiroz, and P. S. Rodrigues da Silva, arXiv:1207.3699.
[18] F. Pisano and V. Pleitez, Phys. Rev. D **46**, 410 (1992); P. H. Frampton, Phys. Rev. Lett. **69**, 2889 (1992); R. Foot, H. N. Long, and T. A. Tran, Phys. Rev. D **50**, R34 (1994);
[19] A. G. Dias, C. A. de S. Pires, and P. S. Rodrigues da Silva, Phys. Lett. B **628**, 85 (2005).
[20] P. V. Dong and H. N. Long, Phys. Rev. D **77**, 057302 (2008); D. Cogollo, A. V. de Andrade, F. S. Queiroz, and P. R. Teles, Eur. Phys. J. C **72**, 2029 (2012); F. Queiroz, C. A. de S. Pires, and P. S. Rodrigues da Silva, Phys. Rev. D **82**, 065018 (2010); A. G. Dias and V. Pleitez, Phys. Rev. D **80**, 056007 (2009); W. A. Ponce, Y. Giraldo, and L. A. Sanchez, Int. J. Mod. Phys. A **21**, 2217 (2006); C. A. de S.

Pires, F. S. Queiroz, and P. S. Rodrigues da Silva, Phys. Rev. D **82**, 105014 (2010).

[21] A. Alves, E. Ramirez Barreto, A. G. Dias, C. A. de S. Pires, F. S. Queiroz, and P. S. Rodrigues da Silva, Phys. Rev. D **84**, 115004 (2011).

[22] J. K. Mizukoshi, C. A. de S. Pires, F. S. Queiroz, and P. S. Rodrigues da Silva, Phys. Rev. D **83**, 065024 (2011); C. A. de S. Pires and P. S. Rodrigues da Silva, J. Cosmol. Astropart. Phys. 12 (2007) 012.

[23] H. Cardenas, D. Restrepo, and J.-A. Rodriguez, arXiv:1205.5726; F. de Campos, O. J. P. Eboli, M. B. Magro, D. Restrepo, and J. W. F. Valle, Phys. Rev. D **80**, 015002 (2009).

[24] G. Belanger, F. Boudjema, A. Pukhov, and A. Semenov, Comput. Phys. Commun. **176**, 367 (2007); G. Belanger, F. Boudjema, A. Pukhov, and A. Semenov, Comput. Phys. Commun. **180**, 747 (2009); G. Belanger, F. Boudjema, A. Pukhov, and A. Semenov, arXiv:1005.4133.

[25] N. Jarosik *et al.*, Astrophys. J. Suppl. Ser. **192**, 14 2011.

[26] L. L. Honorez and C. E. Yaguna, J. High Energy Phys. 09 (2010) 046; L. L. Honorez and C. E. Yaguna, J. Cosmol. Astropart. Phys. 01 (2011) 002.

[27] O. Y. Gnedin, D. Ceverino, N. Y. Gnedin, A. A. Klypin, A. V. Kravtsov, R. Levine, and D. Nagai, G. Yepes, arXiv:1108.5736; O. Y. Gnedin, A. V. Kravtsov, A. A. Klypin, and D. Nagai, Astrophys. J. **616**, 16 (2004).

[28] CMS collaboration, Phys. Lett. B **713**, 68 (2012).

[29] M. Farina, D. Pappadopulo, and A. Strumia, Phys. Lett. B **688**, 329 (2010); Y. Mambrini, Phys. Rev. D **84**, 115017 (2011); Y. Mambrini, arXiv:1112.0011; D. A. Sierra, J. Kubo, D. Restrepo, D. Suematsu, and O. Zapata, Phys. Rev. D **79**, 013011 (2009).

[30] CMS Collaboration, Phys. Lett. B **716**, 30 (2012); ATLAS Collaboration, Phys. Lett. B **716**, 1 (2012).

[31] CDF and DO Collaborations arXiv:1203.3774; CDF and D0 Collaborations arXiv:1203.3782; CMS and ATLAS Collaborations, Phys. Lett. B **710**, 49 (2012); ATLAS Collaboration, Phys. Rev. Lett. **108**, 111803 (2012).